CROP CLASSIFICATION AND SPECTRAL BAND ANALYSIS USING PRISMA HYPERSPECTRAL DATA

Matei Debu, Mihai Ivanovici

ISOP Research Laboratory
Transilvania University of Brașov, Romania

ABSTRACT

Crop classification plays an important role in supporting sustainable agriculture. Hyperspectral data can improve crop classification due to the large amount of spectral information they provide. In this study, we perform crop classification using the HyDACI6 PRISMA hyperspectral dataset and a one-dimensional residual neural network. We compare Normalized Difference Vegetation Index (NDVI) time series with the full spectral information and analyze the contribution of individual spectral bands to classification performance. The widely-used NDVI-based approach achieved an overall accuracy of 70.30%, while using all 187 spectral bands increased the accuracy to 87.00%. The analysis of the contribution of each band to the overall classification accuracy identified the green and red-edge regions as providing the largest contribution. Combining NDVI with only two spectral bands, centered at 550.9 nm and 713.7 nm, achieved an overall accuracy of 84.5%, indicating that a reduced number of spectral bands can retain most of the classification performance provided by the full spectral information.

***Index Terms*—** PRISMA, hyperspectral data, NDVI, crop classification, ResNet.

1. INTRODUCTION

Sustainable agriculture has become increasingly important due to the growing demand for food and the impacts of climate change. Smart Agriculture addresses these challenges by integrating Earth Observation (EO) data with Artificial Intelligence (AI) models to support sustainable agricultural production [1]. EO data have been used for applications such as crop classification, crop monitoring and yield prediction. Crop classification remains challenging when crops exhibit similar spectral and phenological characteristics. As a result, numerous EO-based methods have been developed to improve crop discrimination and classification performance, such as approaches based on vegetation indices derived from Sentinel-2 imagery [2] and data fusion methods that combine multi-spectral Sentinel-2 and radar Sentinel-1 data to enhance crop classification accuracy [3] [4]. A computer vision approach for crop classification is presented in [5], where the authors exploit the spatial characteristics of spectral data by using 32×32 patches derived from Sentinel-2 and Sentinel-1 data as input to a residual network. In [6], several deep learning models were compared for crop classification using multi-temporal Sentinel-2 data, with 3D-CNN achieving the highest accuracy. Similarly, [7] used Sentinel-2 time series with a 3D-CNN for in-season crop mapping.

Hyperspectral imaging is widely used in various domains, including EO, agriculture, forestry and cultural heritage [8]. Previous studies have explored the use of hyperspectral data for crop classification. In [9], a binary crop classification between tomato and corn using hyperspectral data from PRISMA and airborne imagery was presented. The authors used a one-dimensional convolutional neural network to classify the two crops across seven agricultural fields. Another study proposed a deep learning approach that combines hyperspectral information with vegetation indices to improve the discrimination between different crop types [10]. The authors in [11] presented a crop classification approach based on hyperspectral imagery that achieved high classification performance on two hyperspectral datasets.

In this paper, we address crop classification using PRISMA hyperspectral data by comparing Normalized Difference Vegetation Index (NDVI) time series with the full spectral information. Additionally, we analyze the contribution of individual spectral bands and investigate whether a reduced set of selected bands can retain the classification performance of the full hyperspectral data. Reducing the number of spectral bands may simplify the required sensing configuration and reduce the computational complexity of subsequent data processing, while retaining most of the classification performance. The same residual network (ResNet) is used for all experiments.

The paper is structured as follows. Section II presents the hyperspectral data used. Section III presents the experiments with the used AI model and the approaches followed by the results. Finally, the last section concludes the experiment.

This work was supported by a grant of the Ministry of Research, Innovation and Digitization, CCDI-UEFISCDI, ELIAC (Early Identification of Agricultural Crops) project no. PN-IV-P7-7.1-PED-2024-0375 in PNCDI IV.

2. DATA

In our experiments, we used the HyDACI6[1] hyperspectral satellite dataset presented in [12], which is publicly available on Zenodo. The dataset contains six PRISMA hyperspectral images covering one agricultural season, from March to October 2024. Each image consists of 187 spectral bands and covers agricultural parcels located near Brașov, Romania. The area of interest contains 9 agricultural crop classes, comprising a total of 5937 pixels and 52 parcels. Table 1 presents the agricultural crops used in our experiments and the number of parcels and pixels corresponding to each crop.

Crop name	No. of pixels	No. of parcels
Winter wheat	1271	12
Spring wheat	391	2
Corn	686	11
Peas	386	3
Late potatoes	352	4
Sugar beets	822	7
Alfalfa	49	2
Grassland	720	3
Winter rapeseed	1260	8

Table 1. Number of pixels and parcels for each crop.

From the hyperspectral data, we computed the NDVI for each image, resulting in a time series of six NDVI values for each pixel in the area of interest. The formula used to compute NDVI is $NDVI = \frac{NIR-RED}{NIR+RED}$.

For the PRISMA hyperspectral data, the RED value was computed by averaging the reflectance of spectral bands within the wavelength range [645.9 nm, 684.1 nm], while the NIR value was obtained by averaging the bands within [785.6 nm, 892.1 nm]. This approach is presented in [13]. Figure 1 shows the mean NDVI time series for each crop, where each point represents the average NDVI value of all pixels belonging to that crop on the corresponding hyperspectral image acquisition date. Note that some crops have similar growing seasons and development stages. Consequently, their NDVI time series can exhibit similar temporal patterns, which may lead to confusion during classification.

3. EXPERIMENTS

This section presents the AI model used for crop classification, the data partitioning, training configuration parameters and the evaluation of the model's classification performance.

3.1. AI model

To perform the experiments, we employed a one-dimensional ResNet [14], whose architecture is illustrated in Figure 2. The

[1]https://zenodo.org/records/15830646

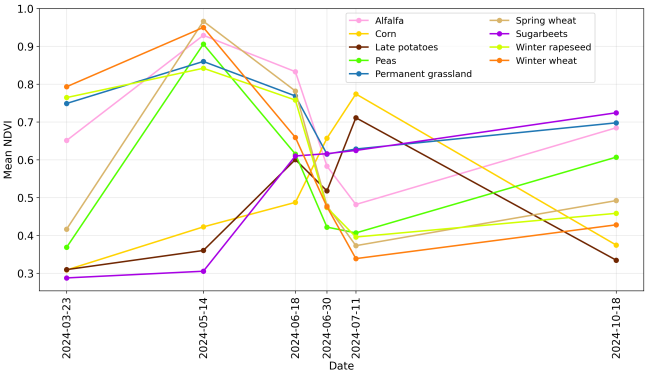


Fig. 1. The NDVI time series for all the crops.

model applies one-dimensional convolutions along the temporal dimension to extract temporal features from the six hyperspectral images. The architecture includes a residual block and combines global average pooling (GAP) and global max pooling (GMP) before the final classification layer. The same network architecture was used for all experiments, while only the input data were changed. In the first experiment, the input consists of the NDVI time series, resulting in an input dimension of 1×6. In the second experiment, all 187 spectral bands from each acquisition date were used, resulting in an input dimension of 187×6. An additional experiment was performed by combining the NDVI time series with each PRISMA spectral band individually to investigate which spectral bands contribute most to the classification performance. The aim of these experiments is to evaluate whether the full spectral information improves crop classification compared with NDVI alone, identify the most relevant spectral regions and investigate whether a reduced set of spectral bands can achieve the same classification performance.

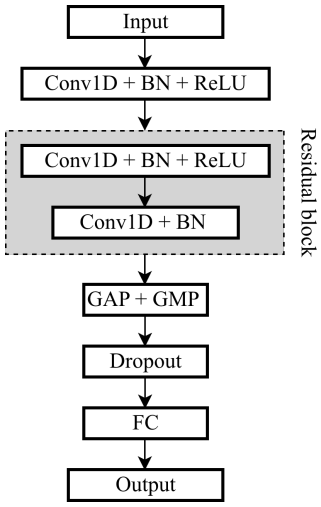


Fig. 2. The proposed architecture for the ResNet 1D.

3.2. Dataset partitioning and training configuration

The dataset was partitioned at the parcel level, such that pixels belonging to the same agricultural parcel were not shared between the training and test sets. A three-fold cross-validation strategy repeated three times was employed, resulting in a total of nine train-test evaluations. The same data partitions were used for all the experiments to ensure a consistent comparison. For each fold, a subset of the training parcels was further used as a validation set for model selection and early stopping. Before training, the input data were standardized using the mean and standard deviation computed from the training data of each fold.

The network was trained using the Adam optimizer with a learning rate of 10^{-3} and a weight decay of 10^{-3}. A cosine annealing learning rate scheduler was employed to gradually decrease the learning rate during training to a minimum value of 10^{-5}. A batch size of 128 and a maximum of 100 epochs were used, with early stopping applied when the validation macro F1-score did not improve for 15 consecutive epochs. A dropout rate of 0.5 was used to reduce overfitting. Weighted cross-entropy was used to address class imbalance.

3.3. Model performance evaluation metrics

The classification performance was evaluated at both pixel and parcel levels. At the pixel level, overall accuracy (OA) and F1-score were used to assess the classification performance. OA represents the proportion of correctly classified pixels over the total number of pixels, while the F1-score provides a balance between precision and recall. Due to the class imbalance in the dataset, the macro-averaged F1-score was also considered, assigning equal importance to each crop class regardless of the number of pixels.

At the parcel level, the predicted class of each agricultural parcel was determined by majority voting over the predictions of all pixels belonging to that parcel. Parcel-level accuracy and macro-averaged F1-score were used to evaluate the classification performance. For the comparison between the NDVI and spectral experiments, the parcel-level macro-averaged F1-score was computed considering only crop classes represented by at least three parcels, ensuring that each evaluated class could be represented across the three-fold cross-validation. Therefore, spring wheat and alfalfa, which contain only two parcels each, were excluded from this metric, but were used in the pixel-level evaluation.

4. RESULTS

4.1. NDVI and full spectral classification

The results of the first experiment are presented in Figure 3. Using the NDVI time series, the model achieved an overall accuracy of 70.30%. The confusion matrix shows that some crop classes exhibit confusion when only the temporal evolution of NDVI is used for classification.

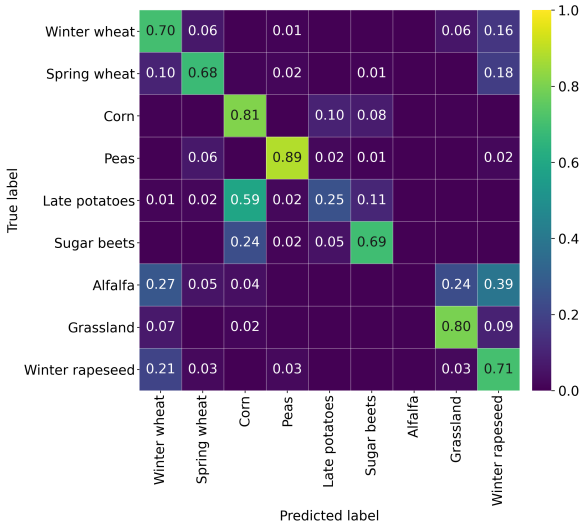


Fig. 3. Pixel-level confusion matrix using NDVI time series.

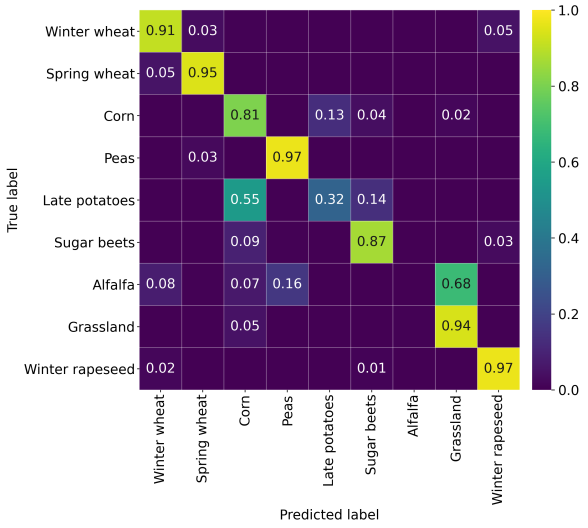


Fig. 4. Pixel-level confusion matrix using all spectral bands.

For the second experiment, all 187 spectral bands from the six hyperspectral images were used. The results of this experiment are presented in Figure 4. The model achieved an overall accuracy of 87.00%. Compared with the NDVI-based experiment, the overall accuracy increased by 16.70 percentage points, showing improved crop discrimination.

The NDVI-based approach shows considerable confusion between winter wheat, spring wheat and winter rapeseed, likely due to their similar growing periods and NDVI temporal patterns (see Figure 1). Using all the spectral bands reduces this confusion, with all three classes achieving accu-

racies above 92%. Confusion is also observed between corn, late potatoes and sugar beets. The spectral approach reduces confusion between sugar beets and corn by almost 15%, and between corn and late potatoes by approximately 4%.

In neither of the two approaches was the model able to accurately classify alfalfa, which was frequently confused with other crop classes. A possible explanation is the very small number of alfalfa pixels available in the dataset. In fact, the crop class with the second-lowest number of pixels contains approximately seven times more pixels than alfalfa.

In addition to the pixel-level evaluation, the performance of the two approaches was also assessed at the parcel level. The NDVI-based experiment achieved a macro-averaged F1 score of $72.2\% \pm 6.7\%$, while the use of the full spectral information increased the score to $81.4\% \pm 10.6\%$. The spectral approach outperformed the NDVI-based approach in eight of the nine cross-validation folds.

4.2. Spectral band analysis

To analyze the contribution of individual spectral bands to crop classification, an additional experiment was performed by combining the NDVI time series with each of the 187 PRISMA spectral bands, one at a time. The results for this experiment are presented in Figure 5. Figure shows that adding spectral information generally improves the classification performance compared with using the NDVI time series alone, with 176 of the 187 bands resulting in a higher OA. Only 11 bands did not improve the OA, mostly at the beginning of the visible spectrum (blue).

The highest classification performance is observed for bands located in two spectral regions. The first region is located in the green part of the spectrum, between approximately 519.5 nm and 583.8 nm, while the second is located in the red-edge region, between approximately 694.1 nm and 723.9 nm. These spectral regions do not overlap with the wavelength ranges used to compute the NDVI, suggesting that they provide complementary spectral information for crop discrimination. The highest OA was obtained when the band centered at 713.7 nm was combined with the NDVI time series, reaching an OA of 83.70%, corresponding to an improvement of 13.41% over the NDVI-only experiment.

4.3. Classification using selected spectral bands

Based on the contribution of the individual spectral bands analyzed, we selected the bands that improved the OA by at least 10% compared with the NDVI-only experiment. The 10% threshold was chosen to exceed the fold-to-fold variability of the NDVI baseline (8.6%). This resulted in a subset of 13 spectral bands located in the green and red-edge regions. In addition, the bands centered at 550.9 nm and 713.7 nm were selected from both regions, as they provided the highest improvements within these two regions. When individually

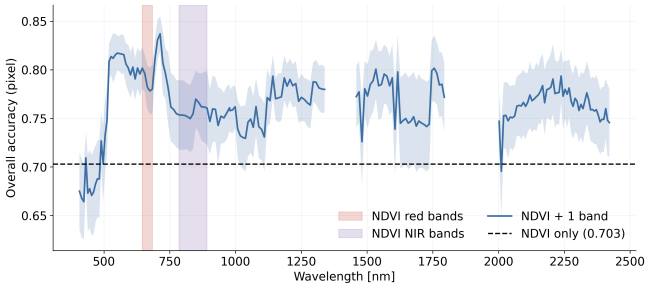


Fig. 5. Pixel-level OA obtained by combining the NDVI time series with each individual PRISMA spectral band.

combined with the NDVI time series, these bands improved the OA by approximately 11% and 13%, respectively. Using these selected bands, additional classification experiments were performed. The results are presented in Table 2 as mean $\pm$ standard deviation over nine evaluations.

The highest pixel-level OA was obtained using all 187 spectral bands ($87.0\% \pm 4.0\%$). Combining NDVI with only the 550.9 nm and 713.7 nm bands achieved $84.5\% \pm 5.1\%$ and the highest parcel-level macro-F1 ($85.8\% \pm 8.3\%$). Using the 13 selected bands achieved an OA of $83.4\% \pm 4.4\%$, while their combination with NDVI reached $82.0\% \pm 7.0\%$. Overall, the two-band configuration retained most of the full spectral performance using only 3 channels and 7,305 parameters, compared with 187 channels and 24,969 parameters.

5. CONCLUSIONS

This study focuses on the classification of nine agricultural crops in the Brașov area, Romania, using PRISMA hyperspectral data from the HyDACI6 dataset. A one-dimensional residual neural network was employed to investigate the contribution of hyperspectral information to crop classification. The use of all 187 spectral bands improved the overall accuracy by 16.70% compared with the NDVI time series, demonstrating the advantage of exploiting the full spectral information for crop discrimination.

Additional experiments were conducted to analyze the contribution of individual spectral bands and identify the spectral regions that provide the most relevant information for crop classification. The spectral band analysis showed that the largest improvements in classification performance were obtained when bands from the green and red-edge regions were combined with the NDVI time series. Using only the bands centered at 550.9 nm and 713.7 nm together with NDVI achieved an overall accuracy of 84.5%, only 2.5% lower than the 87.0% obtained using all 187 spectral bands. These results show that a few selected spectral bands can retain most of the full spectral classification performance while reducing model complexity. The current experiments evaluate the model on unseen agricultural parcels, while all temporal

Input	Channel(s)	Parameters	OA (pixel)	Macro-F1 parcel	Correct parcels
NDVI	1	7113	0.703 ± 0.086	0.722 ± 0.067	43/52
NDVI + 713.7nm	2	7209	0.837 ± 0.054	0.820 ± 0.099	46/52
NDVI + 550.9nm + 713.7nm	3	7305	0.845 ± 0.051	$\mathbf{0.858 \pm 0.083}$	**48/52**
NDVI + 13 selected bands	14	8361	0.820 ± 0.070	0.820 ± 0.051	45/52
13 selected bands	13	8265	0.834 ± 0.044	0.832 ± 0.072	47/52
All 187 spectral bands	187	24969	$\mathbf{0.870 \pm 0.040}$	0.814 ± 0.106	46/52

Table 2. Classification performance obtained using different combinations of NDVI and selected PRISMA spectral bands.

observations are known. Generalization to completely unseen time series could not be directly assessed. Additional PRISMA or EnMAP acquisitions for the study area will allow us to evaluate the model on new observations from different acquisition dates and assess its temporal generalization.

6. REFERENCES

[1] M. Ivanovici, G. Olteanu, C. Florea, R.-M. Coliban, M. Ștefan, and K. Marandskiy, "Digital transformation in agriculture," in *Digital Transformation: Exploring the Impact of Digital Transformation on Organizational Processes*, pp. 157–191. Springer, 2024.

[2] R. Sonobe, Y. Yamaya, H. Tani, X. Wang, N. Kobayashi, and K. Mochizuki, "Crop classification from Sentinel-2-derived vegetation indices using ensemble learning," *Journal of Applied Remote Sensing*, vol. 12, no. 2, pp. 026019, 2018.

[3] C. Raab, V. D. Nguyen, B. Barrett, A. Zakirova, M. Zuberi, H. Alff, and M. Spies, "Crop type classification in smallholder agriculture of central and south asia using sentinel-1/2 data fusion," *Remote Sensing Applications: Society and Environment*, p. 102007, 2026.

[4] G. Cheng, H. Ding, J. Yang, and Y. Cheng, "Crop type classification with combined spectral, texture, and radar features of time-series sentinel-1 and sentinel-2 data," *International Journal of Remote Sensing*, vol. 44, no. 4, pp. 1215–1237, 2023.

[5] A. Băicoianu, I. C. Plajer, M. Debu, M. Ștefan, M. Ivanovici, C. Florea, A. Cațaron, R. M. Coliban, S. Popa, S. Oprișescu, A. Racovițeanu, Gh. Olteanu, K. Marandskiy, A. Ghinea, A. Kazak, L. Majercsik, A. Manea, and L. Dogar, "Dacia5: a sentinel-1 and sentinel-2 dataset for agricultural crop identification applications," *Big Earth Data*, vol. 9, no. 4, pp. 1226–1257, 2025.

[6] Q. Li, J. Tian, and Q. Tian, "Deep learning application for crop classification via multi-temporal remote sensing images," *Agriculture*, vol. 13, no. 4, 2023.

[7] I. Gallo, L. Ranghetti, N. Landro, R. La Grassa, and M. Boschetti, "In-season and dynamic crop mapping using 3d convolution neural networks and sentinel-2 time series," *ISPRS Journal of Photogrammetry and Remote Sensing*, vol. 195, pp. 335–352, 2023.

[8] D. Hong, C. Li, N. Yokoya, B. Zhang, X. Jia, A. Plaza, P. Gamba, J. A. Benediktsson, and J. Chanussot, "Hyperspectral imaging," *Nature Reviews Methods Primers*, vol. 6, no. 1, pp. 19, 2026.

[9] D. Spiller, L. Ansalone, F. Carotenuto, and P. P. Mathieu, "Crop type mapping using prisma hyperspectral images and one-dimensional convolutional neural network," in *2021 IEEE International Geoscience and Remote Sensing Symposium IGARSS*, 2021, pp. 8166–8169.

[10] S. Zhang, Y. Jiang, C. Wang, W. Liu, D. Li, and K. Wu, "Crop type classification network for hyperspectral images coupled with agricultural vegetation indices," in *2023 11th International Conference on Agro-Geoinformatics (Agro-Geoinformatics)*, 2023, pp. 1–6.

[11] M. Alajmi, H. A. Mengash, M. M. Eltahir, M. Assiri, S. S. Ibrahim, and A. S. Salama, "Exploiting hyperspectral imaging and optimal deep learning for crop type detection and classification," *IEEE Access*, vol. 11, pp. 124985–124995, 2023.

[12] M. Debu, K. Marandskiy, S. Oprisescu, and M. Ivanovici, "A prisma-based hyperspectral dataset for agriculture," in *2025 15th Workshop on Hyperspectral Imaging and Signal Processing: Evolution in Remote Sensing (WHISPERS)*, 2025, pp. 1–5.

[13] I. C. Plajer, A. Băicoianu, L. Majercsik, and M. Ivanovici, "Ndvi computation from hyperspectral images," in *2023 13th Workshop on Hyperspectral Imaging and Signal Processing: Evolution in Remote Sensing (WHISPERS)*, 2023, pp. 1–5.

[14] K. He, X. Zhang, S. Ren, and J. Sun, "Deep residual learning for image recognition," in *2016 IEEE Conference on Computer Vision and Pattern Recognition (CVPR)*, 2016, pp. 770–778.